Deuteron-deuteron fusion in laser-driven counter-streaming collisionless plasmas

Xiaopeng Zhang,[1] Jiarui Zhao,[2] Dawei Yuan,[3] Changbo Fu,[1,*] Jie Bao,[4] Liming Chen,[2,5] Jianjun He,[6] Long Hou,[4] Liang Li,[1] Yanfei Li,[2] Yutong Li,[2,5,†] Guoqian Liao,[2] Yongjoo Rhee,[7] Yang Sun,[1,5] Shiwei Xu,[6] Gang Zhao,[3] Baojun Zhu,[2] Jianqiang Zhu,[8] Zhe Zhang,[2] and Jie Zhang[1,5]

[1]*School of Physics and Astronomy, Shanghai Jiao Tong University, Shanghai 200240, China*
[2]*Laboratory of Optical Physics, Institute of Physics, Chinese Academy of Sciences, Beijing 100190, China*
[3]*National Astronomical Observatories, Chinese Academy of Sciences, Beijing 100012, China*
[4]*Department of Nuclear Physics, China Institute of Atomic Energy, Beijing 102413, China*
[5]*IFSA Collaborative Innovation Center, Shanghai Jiao Tong University, Shanghai 200240, China*
[6]*Institute of Modern Physics, Chinese Academy of Sciences, Lanzhou 730000, China*
[7]*Nuclear Data Center, Korea Atomic Energy Research Institute, Daejon 305353, Korea*
[8]*Shanghai Institute of Optics and Fine Mechanics, Chinese Academy of Sciences, Shanghai 201800, China*

(Received 8 November 2016; revised manuscript received 15 April 2017; published 1 November 2017)

Nuclear fusion reactions are the most important processes in nature to power stars and produce new elements, and lie at the center of the understanding of nucleosynthesis in the universe. It is critically important to study the reactions in full plasma environments that are close to true astrophysical conditions. By using laser-driven counter-streaming collisionless plasmas, the fusion $d + d \rightarrow {}^3\mathrm{He} + n$ is studied in a Gamow-like window around 27 keV. The results give hints that astrophysical nuclear reaction yields can be modulated significantly by the self-generated electromagnetic fields and the collective motion of the plasma. This plasma-version minicollider may provide a novel tool for studies of astrophysics-interested nuclear reactions, as well as a useful tool to constrain the models of plasma colliding dynamic.

DOI: 10.1103/PhysRevC.96.055801

I. INTRODUCTION

Collisionless plasma (CLP) exists in many astrophysical environments. Well-known examples of CLPs are widely found collisionless shockwaves in supernovae remnants, in γ-ray bursts, and in solar winds, etc. [1]. Though called "collisionless", collisions can occur between the nuclei in CLPs with low probabilities, resulting in nuclear reactions. In these special environments, nucleosynthesis could be significantly different from that in usual cases mainly due to the following facts. Firstly, the energy distribution of the particles in a CLP may be far from thermal equilibrium. Due to the "collisionless" features, the particle density in CLPs is typically very low and the velocities of the particles are very high, and consequently, the particle's mean free path is normally much larger than its dynamic transition length [2]. Therefore, some charged particles in it can be continuously accelerated in a large scale without losing their energy too much through scattering [3], and the system can keep in nonthermal equilibrium for a long time. Secondly, the self-generated macroscale electromagnetic field, originating from the effects such as the Biermann battery effect and the Weibel instability [4], can affect the motion of the particles, and thus their nuclear reaction yield. Lastly, the reaction yield could be significantly modified by the so-called electron screening effect [5]. For nuclei in the normal atomically bound states, their decay properties and reaction rates can be completely different from those in plasma environments [6,7]. However, almost all nuclear parameters used as astrophysical inputs are traditionally measured under nonplasma environments. Obviously, the creation of plasma conditions in terrestrial laboratories for studying astrophysical nuclear reactions is critically important, and may help to solve some longstanding nucleosynthesis puzzles, for instance, the puzzles on ^{26}Al [8] and ^{6,7}Li abundance [9].

The development of high-intensity laser technologies makes it possible to create plasma environments for nuclear studies in earth-based laboratories [10]. When intense laser beams are focused onto targets, they can produce exotic conditions similar to some astrophysical environments, in which nuclear reactions are ignited.

It has been proved that CLPs can be created by high-intensity lasers [11]. The dynamics of CLPs has been studied for over one decade and is still a vivid research area today [12–18]. However, observation of nuclear reactions in laser-induced CLPs has been rarely reported [19]. Several experimental methods for nuclear studies based on high-intensity lasers have been developed in recent years, for example, the Coulomb explosion method [20–22], the inertial confined fusion method [23], and the double lasers method [24]. However, these methods have limitations such as untunable energy and the need for a large facility, etc.

In this paper, we report the studies of $^2\mathrm{H}(d,n)^3\mathrm{He}$ for the first time in a CLP by using laser-driven head-on-head collision of plasma streams. Because of the head-on-head collision, there is an enhancement of the center-of-mass (c.m.) energy by a factor of four. The reaction yields are thereby significantly enhanced as the reaction cross section increases exponentially with the c.m. energy. We show that this kind

*Corresponding author: cbfu@sjtu.edu.cn
†Corresponding author: ytli@iphy.ac.cn

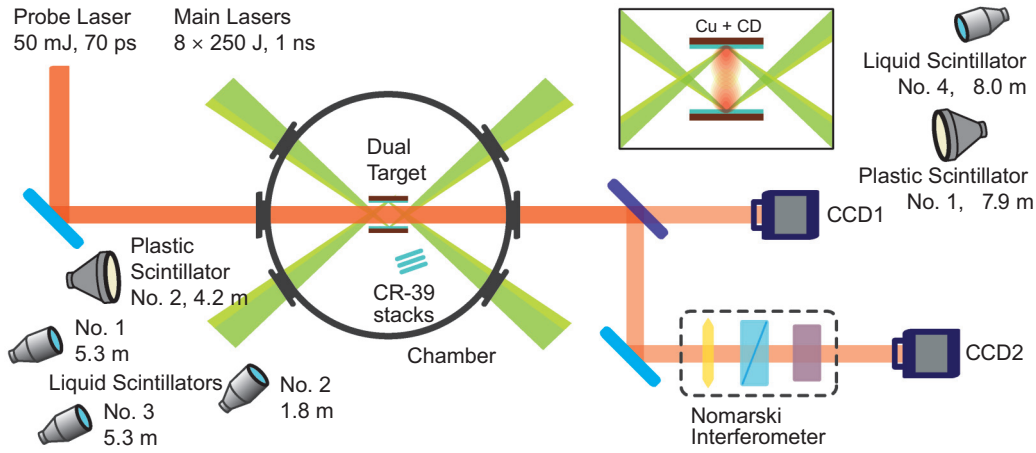

FIG. 1. The experimental setup. Four laser beams were tuned to focus on the target at one side and another four on the opposite side. By using the probe laser and a Nomarski interferometer, the optical images of the plasmas were taken. Neutron signals were recorded by scintillation detectors at different distances.

of miniplasma collider [25,26] has potential applications for studying astrophysical nuclear reactions in earth-based laboratories with features like tunable energies to cover the Gamow window [5].

II. EXPERIMENTAL SETUP

The experiment was performed at the Shenguang II laser facility, in the National Laboratory on High Power Lasers and Physics, Shanghai, China. The experimental setup is shown in Fig. 1. There were eight laser beams at this facility, each of which could deliver an energy of about 250 J with a pulse width of 1 ns at a wavelength of 351 nm (3ω). Two targets were located at the center of the laser chamber. Both of the targets had 0.5×0.5 mm^2 sized copper bases which were coated with 10 μm thick deuterated hydrocarbon ($CD_{1.29}$) layers and a separation of 4.4 mm between them [27]. The main lasers were arranged as two sets $(4 + 4)$, and each set had four lasers focusing on one of the targets. The diameter of the focal spots was about 150 μm, producing a laser intensity of about 6×10^{15} W/cm^2.

Another laser with a duration of 70 ps and wavelength of 526 nm was used as the probe, which passed through the plasma generated by the main laser beams. The interference images were taken by a Nomarski interferometer [28,29]. By tuning the delay time between the probe laser and the main lasers, snapshots of the plasma at different times could be taken.

Scintillation detectors were located outside the laser target chamber. Four of them were liquid scintillators (EJ-301) with a size of $(\pi/4) \times 12.7^2 \times 12.7$ cm^3, along with two plastic scintillators (BC400) with a size of $(\pi/4) \times 25.4^2 \times 5$ cm^3. All scintillators were directly coupled with photomultiplier tubes (PMTs). The signals were recorded by oscilloscopes with a bandwidth of 1 GHz. A stack of nuclear track detector CR-39 sheets with a dimension of $5 \times 5 \times 1$ mm^3 was placed 10 cm away from the targets for neutron dosimetry. The sheets were wrapped in aluminum foils to get rid of the low-energy ions.

III. RESULTS AND ANALYSIS

Neutrons were measured by the time-of-flight (TOF) approach from the scintillators. Typical TOF spectra are shown in Fig. 2, in which the results from four liquid scintillation detectors at different locations are given. In each of the curves, the first dip to the left, which saturates the detectors, represents the photons induced by the high-intensity lasers. The photons, including x rays and γ rays, are induced by the original 351 nm, 1 ns width laser pulse and scattered secondary photons on the materials around the targets. Since most x-ray and γ-ray emissions in atoms or nuclei are in a smaller-than 1 ns domain, they are expected to arrive at the detectors as a ns-width pulse, which is the same pulse width as the original driving laser.

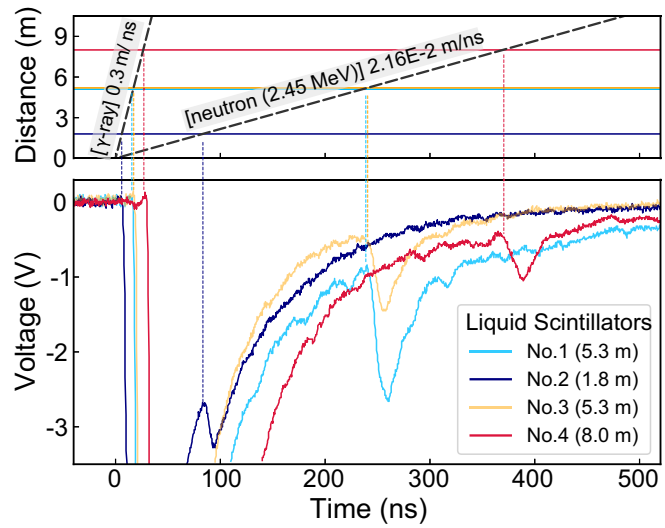

FIG. 2. Typical TOF spectra of neutron detectors. Data from the four liquid scintillation detectors at distances of 5.3 m, 1.8 m, 5.3 m, and 8.0 m, are shown in the lower panel. The expected arriving times of photons and neutrons (2.45 MeV) for each detector are indicated by dashed lines in the upper panel. They match well with the TOFs measured by detectors at different distances.

TABLE I. Experimental condition and measured neutron yield for each run.

Run#	Lasers	Laser energy (J)	Target 1	Target 2	Neutron yield
34	4+4	297 × 8	CD	CD	$(3.8 \pm 1.1) \times 10^5$
35	4+0	260 × 4	CD	-	0
36	4+4	254 × 8	CD	CD	$(4.0 \pm 1.2) \times 10^5$
37	4+4	244 × 8	CD	CD	$(3.9 \pm 1.1) \times 10^5$
38	4+4	254 × 8	CD	Cu (only)	0
39	4+4	217 × 8	CD	Cu (only)	0
40	4+4	246 × 8	CD	Cu (only)	0
79	4+4	230 × 8	CD	CD	$(1.0 \pm 0.5) \times 10^5$
80	4+0	263 × 4	CD	CD	$(0.5 \pm 0.3) \times 10^5$
81	4+0	219 × 4	CD	CD	$(0.6 \pm 0.3) \times 10^5$

Within such a narrow width, the photons are highly overlapped, and some detectors may be saturated. The long tail of the first dip is due to the long discharging time of the PMTs.

The second dip in the curves in Fig. 2 represents the neutron products. The neutrons from the ^{2}H$(d,n)^3$He reaction have an energy of $E_n = 2.45$ MeV, or a speed of 2.16 cm/ns, which is much smaller than that of the photons (30 cm/ns). The expected neutron speed and the measured neutron speeds at different detector locations show good agreement with each other.

To obtain absolute neutron yields, all detectors have been calibrated by using a D-D [where 'D' denotes 'deuterium (^{2}H)'] neutron generator and a ^{137}Cs γ-ray source. The Monte Carlo (MC) simulation code, GEANT4 [30], is employed for the calibration. In the MC simulation, after the to-be-detected particles deposit energies in the scintillator, the energy is transferred to luminescent photons with different efficiencies for neutrons and γ rays [31].

The final neutron yields for different runs are obtained by combining the MC simulation, the experimental calibration data of the ^{137}Cs γ source and the neutron generator, as well as weighted values of all the detectors. The results are shown in Table I. The neutron yields in runs with a head-on collision scenario (Runs 34–37) are on the order of 10^5. Run 79 has the same target configuration to Runs 34–37, while its neutron yield is about 3σ away from the average. This is due to an unexpected laser condition caused by a faulty aiming operation.

There could be only a few neutrons expected on a detector at distance of 10 m when the neutron yield is 10^5. This caused large fluctuations to the neutron yield results. It can be seen from Table I that the neutron yields measured have large uncertainties especially for those runs which have a smaller yield (Runs 79–81). Several measures could be adopted to reduce the fluctuations in future experiments. In addition to larger detecting solid angles, if detectors were shielded by lead bricks to reduce the original photon shower, a higher voltage can be applied to the detectors, and a higher detection efficiency may be achieved.

From the CR-39 detectors, no significant signal above background was found. The detecting sensitivity of CR-39 for fast neutrons is of order 10^{-4} [32], which sets an upper limit of 10^6 neutrons per shot in this work [27].

The observed neutrons might come from three sources: from the original laser-induced fireballs ($N_{\rm fb}$), from the cold target when the energetic deuterium ions from the opposite target hit it ($N_{\rm cold}$), and from the area where two plasma currents collide with each other ($N_{\rm collide}$). The total neutron yield is the sum of all the three sources, i.e., $N_{\rm total} = N_{\rm fb} + N_{\rm cold} + N_{\rm collide}$.

To see how many neutrons come from the original fireballs, we either took off the second CD target (Table I, Run 35) or left only a target base without CD film on it (Table I, Runs 38–40), while keeping all other laser parameters the same. The results have shown no evidence of neutrons from those runs, i.e., under the detecting limit of $<2 \times 10^3$ (95% C.L.).

To determine $N_{\rm cold}$, four lasers were focused on one of the two CD targets, but no laser directly focused on the opposite one. The neutron yields for this setup were about 0.5×10^5 (Table I, Runs 80 and 81), which were much smaller than the cases with double targets (Runs 34–37). Moreover, it should be noted that the second target in Runs 80 and 81 was not totally "cold". Since this target was only 4.4 mm away from the opposite one, it has been ionized by the scattered laser and the x ray coming from the opposite target [33,34]. In fact, plasma on the opposite target surface was observed on the interferometer images in these runs. We suspect that there would be a much smaller $N_{\rm cold}$ for a complete cold target situation.

Comparing the measured $N_{\rm fb}$, $N_{\rm cold}$, and $N_{\rm collide}$, one can conclude that the neutron yields are dominated by $N_{\rm collide}$ contribution, and the present setup provides an efficient way to ignite nuclear fusion reactions in a minisize collider.

The Abel inversion approach has been employed to deduce the electron density n_e. Since the spatial distribution of the plasma is not ideally symmetrical, we followed a numerical method for the asymmetrical Abel inversion described in Ref. [35]. For the $CD_{1.29}$ targets used in the experiment, considering the charge neutrality of plasma in the μm scale and the fact that the carbon and deuteron atoms were fully ionized in the energy range of interest (>5 keV), the density of deuterons in the plasma can be estimated as

$$n_{\rm D} \approx \frac{1.29}{6 + 1.29} n_e. \tag{1}$$

A typical density distribution is shown in Fig. 3. From the data, one can estimate the collision frequency between electrons (e-e), electrons and deuteron ions (e-D), and D-D. The D-D mean free path, $\lambda_{\rm DD}$, can be written as [36]

$$\lambda_{\rm DD} = \frac{m_{\rm D}^2 v_{12}^4}{4\pi Z^4 e^4 n_{\rm D} \ln \Lambda_{12}}, \tag{2}$$

where $m_{\rm D}$ is the deuteron mass, v_{12} the relative velocity, Ze the ion's charge, and $\ln \Lambda_{12}$ the so-called "Coulomb logarithm" [37]. With our experimental setup, in the relative velocity range $v_{12} > 1 \times 10^8$ cm/s (corresponding to $E_{\rm c.m.} > 5.2$ keV), $\lambda_{\rm DD}$ is calculated to be larger than 46 mm, which is much larger than the separation between the two targets (4.4 mm). Therefore, the plasma is really "collisionless" for a deuteron energy larger

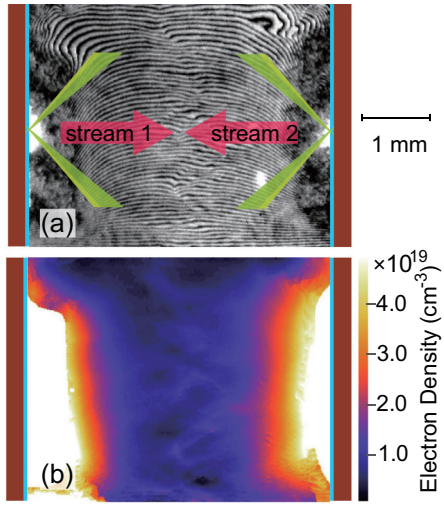

FIG. 3. (a) A typical Nomarski interferogram of the plasma streams, and (b) the corresponding electron density distribution derived by Abel inversion approach.

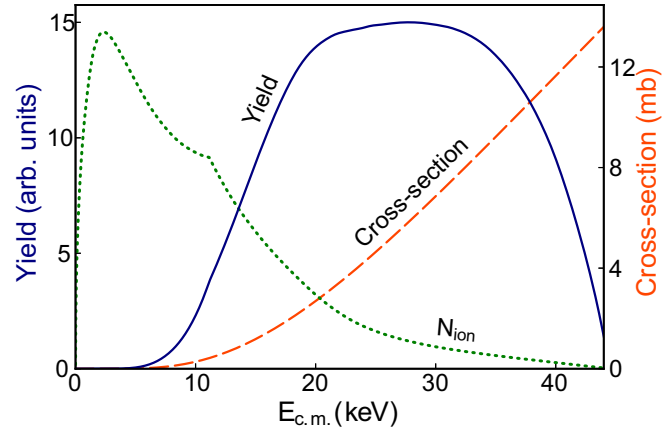

FIG. 4. The Gamow-window-like feature of the neutron yield contributed by deuterium ions with different c.m. energies. Three lines are shown in this chart: the number of the ions from the experimental data (the dotted green line), the ^{2}H$(d,n)^3$He cross section (the dashed red line), and the calculated neutron yield (the solid blue line).

than 5.2 keV. The e-D collision frequency of 3×10^{10}/s can also be estimated. This means the electrons could collide with other electrons and ions about 30 times in 1 ns. Consequently, a quasithermal equilibrium of ions is established, i.e., the ion energy distribution is quasi-Boltzmann, and the ion number drops exponentially as the energy increases.

It is worth pointing out that only the front part of the expanding plasma is "collisionless plasma". Even if this part is "collisionless", the ions in it still have a relatively small chance of colliding with each other and induce nuclear reactions.

A numerical calculation has been carried out with a simplified plasma dynamic model to obtain the expected neutron yields. Considering the fact that $N_{\rm fb}$ is very small, we assume the deuterons from one target can only have reactions with those from the opposite side, and the D-D neutrons from the same side are negligible. The reaction yield can be written as

$$Y = \iiint n_{1\rm D}(\mathbf{r}_1,t)\, n_{2\rm D}(\mathbf{r}_2,t)\sigma(v_1,v_2)\mathrm{d}\mathbf{r}_1\mathrm{d}\mathbf{r}_2\mathrm{d}S, \quad (3)$$

where $n_{1\rm D}$ and $n_{2\rm D}$ are the deuteron densities of the left and right sides, respectively, and S is the section area of the fluxes. The deuteron density, as a function of time and position, is calculated according to Eq. (1), while the electron density is calculated by MULTI2D [27,38].

The cross section is

$$\sigma(E_{\rm c.m.}) = S(E_{\rm c.m.})\exp(-2\pi\eta)/E_{\rm c.m.}, \quad (4)$$

where $E_{\rm c.m.} = \frac{m}{4}(v_1+v_2)^2$ is the c.m. energy, $S(E_{\rm c.m.})$ defined by this equation is the astrophysical S factor, and $\eta = \frac{Z_1 Z_2 e^2}{\hbar(v_1+v_2)}$ is the Sommerfeld parameter.

We have simplified the ion speed v as a constant in the collisionless regime, i.e., $v = z/t_0$, where t_0 is the delayed time of the probe laser, and z is the distance to the target. The deuteron density $n_{\rm D}$ is separated into left and right parts which are originally from the left and right targets, respectively, i.e., $n_{\rm D} = n_{1\rm D} + n_{2\rm D}$.

Figure 4 shows the D-D reaction yield for different velocities in plasma with the assumptions described above. One can find that the number of ion pairs ($N_{\rm ion}$) decreases as $E_{\rm c.m.}$ increases (dotted green line), while the cross section increases as $E_{\rm c.m.}$ increases (dashed red line). Therefore, according to Eq. (3), large reaction yields are found in the c.m. energy ranging from 15 to 40 keV, as shown by solid blue line in Fig. 4. This Gamow-window-like structure implies that the present method could be a promising new tool for key reactions with nuclear-astrophysical interest, which are otherwise very difficult, if not impossible, to perform in traditional experimental setups.

The calculated neutron yield using the simplified model is $(3.1 \pm 1.2) \times 10^6$ for Run 37, or 8 times larger than the experimental observation. This disagreement is mainly due to the neglected self-generated magnetic fields in our calculation, as well as our oversimplified model. With the current experimental conditions, the head-on-head collision of plasma streams can generate a toroidal field inversely proportional to electron density and the distance to the symmetrical axis, i.e., $B_\phi/n_e r = \text{const}$ [39]. This type of field has been reported in previous experiments with a similar head-on-head collision setup [11,17], and the magnetic field strength is estimated to be about 10 T level. Under this field strength, the deuterons with an energy of tens keV can be significantly bent from a straight path. Therefore, the c.m. energy of the ion pairs should become smaller, thus resulting in a smaller neutron yield.

The density and velocity distributions of ions in the plasma and their time evolution are critical in evaluating how many ions involved in nuclear reactions and their reaction cross sections. The data quality could be improved by increasing the energy and contrast of the probe laser used in the interferometry diagnostics. Furthermore, if taking more interferograms at different moments and from multiple directions, a higher accuracy could be achieved. Other diagnostic methods including Faraday cups [40] are also under testing for the future experiments.

IV. IMPLICATIONS FOR NUCLEAR ASTROPHYSICS

The method introduced in this article could have far-reaching implications for future nuclear reaction experiments that aim to understand the origin of element production in the universe.

First, this method provides a controllable way to trigger nuclear reactions within the Gamow window. Traditional accelerators have very low peak beam intensities and result in a very low signal-to-background noise ratio. Therefore, due to the extremely low cross sections, it is very difficult to study nuclear reactions in their Gamow windows with traditional accelerators. Quasi-Boltzmann spectra can be obtained in the Coulomb explosion setup [20], but its temperature is determined by the distance and the Coulomb force between nuclei and is hardly tunable. By tuning the laser intensity (changing the total laser energy, the pulse width, or the focal spot size), ions which are involved in the nuclear reaction (in the Gamow-like window) could be tuned [41]. This is the only reported method that can provide particles with a controllable quasi-Boltzmann distribution for nuclear astrophysical studies to the best of our knowledge.

Second, this setup provides a laboratory-based full plasma environment for nuclear reactions studies. There have been strong indications that decay properties and reaction rates of bare nuclei in plasmas differ significantly from those of atomically bound states obtained from normal conditions [6,7]. Compared with other methods, for example the Coulomb explosion method [20] or the storage ring method [42], the plasma in this work is charge neutral, and the environment created here is more similar to that of real astrophysical cases.

Third, the results show hints that the self-generated macroscale electromagnetic field may play an important role in the nucleosynthesis of our universe. A plasma in a "collision" state means that ions in it collide with each other frequently so that the system can quickly reach a thermal equilibrium; while a "collisionless" state means the ions rarely collide, and the system is far from a thermal equilibrium. Because of the collisionless features, the nuclei inside CLPs can process in macroscale lengths before being scattered, and thus acquire energy due to the self-generated, macroscale electrical field [14]. The nuclei can be accelerated or deflected, and therefore the reaction yields could be completely different from those in thermal equilibriums, as observed in this experiment. These nuclear reaction studies in a laboratory CLP may be important in solving the long-standing puzzles like the ^{6,7}Li abundance in big bang nucleosynthesis.

V. SUMMARY

We have presented a novel experimental method for studying nuclear reactions in plasma environments. Taking advantage of the extremely high ion flux and high temperatures induced by lasers, stellar environments could be simulated, in which low energy and small cross-section nuclear reactions could be studied in earth-based laboratories. By employing this method, ^{2}H$(d,n)^{3}$He reactions were realized by using head-on-head collision of plasma streams driven by nanosecond pulse lasers. The experimental results have shown that the neutron yield from the nuclear reactions is enhanced significantly by the head-on-head collision of two beams compared to the case of beam-on target collisions, benefited from an increase in the c.m. energy. We have also found evidence that the self-generated electromagnetic fields in CLPs might significantly affect the nuclear reaction yield. With an improved plasma flux and a magnetic structure diagnosis, this novel plasma-version minicollider may be employed in fields like nuclear astrophysical processes and the magnetic confinement fusion in the near future.

ACKNOWLEDGMENTS

We would like to acknowledge the SG-II staff for operating the laser facility, CAEP staff for the target fabrication. This work is supported by the National Basic Research Program of China (Grants No. 2013CBA01501 and No. 2013CB834401), the National Science Foundation of China (Grants No. 11135012, No. 11135005, and No. 11375114), Science Challenge Project (Grant No. TZ2016005), and the Global R&D Networking Program funded by the Republic of Korea's Ministry of Science, ICT and Future Planning (Grant No. NRF-2012-0004839). One of us (C.B.F.) thanks Science and Technology Commission of Shanghai Municipality for the support (under Grant No. 11DZ2260700).

[1] D. Biskamp, Collisionless shock waves in plasmas, Nucl. Fusion **13**, 719 (1973).
[2] A. Bret, Collisional behaviors of astrophysical collisionless plasmas, J. Plasma Phys. **81**, 455810202 (2015).
[3] R. Blandford and D. Eichler, Particle acceleration at astrophysical shocks: A theory of cosmic ray origin, Phys. Rep. **154**, 1 (1987).
[4] D. Ryu, D. R. Schleicher, R. A. Treumann, C. G. Tsagas, and L. M. Widrow, Magnetic fields in the large-scale structure of the universe, Space Sci. Rev. **166**, 1 (2012).
[5] C. E. Rolfs and W. S. Rodney, *Cauldrons in the Cosmos: Nuclear Astrophysics* (University of Chicago Press, Chicago, 1988).
[6] Y. A. Litvinov and F. Bosch, Beta decay of highly charged ions, Rep. Prog. Phys. **74**, 016301 (2011).
[7] K. Czerski, A. Huke, A. Biller, M. Hoeft, and G. Ruprecht, Enhancement of the electron screening effect for d + d fusion reactions in metallic environments, Europhys. Lett. **54**, 449 (2001).
[8] N. Prantzos and R. Diehl, Radioactive ^{26}Al in the galaxy: Observations versus theory, Phys. Rep. **267**, 1 (1996).
[9] R. H. Cyburt, B. D. Fields, K. A. Olive, and T. H. Yeh, Big bang nucleosynthesis: Present status, Rev. Mod. Phys. **88**, 015004 (2016).
[10] B. A. Remington, D. Arnett, R. Paul, Drake, and H. Takabe, Modeling astrophysical phenomena in the laboratory with intense lasers, Science **284**, 1488 (1999).
[11] C. K. Li, D. D. Ryutov, S. X. Hu, M. J. Rosenberg, A. B. Zylstra, F. H. Seguin, J. A. Frenje, D. T. Casey, M. GatuJohnson,

M. J.-E. Manuel, H. G. Rinderknecht, R. D. Petrasso, P. A. Amendt, H. S. Park, B. A. Remington, S. C. Wilks, R. Betti, D. H. Froula, J. P. Knauer, D. D. Meyerhofer, R. P. Drake, C. C. Kuranz, R. Young, and M. Koenig, Structure and Dynamics of Colliding Plasma Jets, Phys. Rev. Lett. **111**, 235003 (2013).

[12] Y. Kuramitsu *et al.*, Jet formation in counterstreaming collisionless plasmas, Astrophys. J. Lett. **707**, L137 (2009).

[13] D. D. Ryutov, N. L. Kugland, H.-S. Park, S. M. Pollaine, B. A. Remington, and J. S. Ross, Collisional current drive in two interpenetrating plasma jets, Phys. Plasmas **18**, 104504 (2011).

[14] N. L. Kugland *et al.*, Self-organized electromagnetic field structures in laser-produced counter-streaming plasmas, Nat. Phys. **8**, 809 (2012).

[15] J. S. Ross *et al.*, Characterizing counter-streaming interpenetrating plasmas relevant to astrophysical collisionless shocks, Phys. Plasmas **19**, 056501 (2012).

[16] D. D. Ryutov, N. L. Kugland, H.-S. Park, C. Plechaty, B. A. Remington, and J. S. Ross, Intra-jet shocks in two counter-streaming, weakly collisional plasma jets, Phys. Plasmas **19**, 074501 (2012).

[17] C. M. Huntington *et al.*, Observation of magnetic field generation via the Weibel instability in interpenetrating plasma flows, Nat. Phys. **11**, 173 (2015).

[18] J. S. Ross, D. P. Higginson, D. Ryutov, F. Fiuza, R. Hatarik, C. M. Huntington, D. H. Kalantar, A. Link, B. B. Pollock, B. A. Remington, H. G. Rinderknecht, G. F. Swadling, D. P. Turnbull, S. Weber, S. Wilks, D. H. Froula, M. J. Rosenberg, T. Morita, Y. Sakawa, H. Takabe, R. P. Drake, C. Kuranz, G. Gregori, J. Meinecke, M. C. Levy, M. Koenig, A. Spitkovsky, R. D. Petrasso, C. K. Li, H. Sio, B. Lahmann, A. B. Zylstra, and H. S. Park, Transition from Collisional to Collisionless Regimes in Interpenetrating Plasma Flows on the National Ignition Facility, Phys. Rev. Lett. **118**, 185003 (2017).

[19] D. Mascali *et al.*, Colliding laser-produced plasmas: A new tool for nuclear astrophysics studies, Radiat. Eff. Defects Solids **165**, 730 (2010).

[20] T. Ditmire, J. Zweiback, V. P. Yanovsky, T. E. Cowan, G. Hays, and K. B. Wharton, Nuclear fusion from explosions of femtosecond laser-heated deuterium clusters, Nature **398**, 489 (1999).

[21] M. Barbui, W. Bang, A. Bonasera, K. Hagel, K. Schmidt, J. B. Natowitz, R. Burch, G. Giuliani, M. Barbarino, H. Zheng, G. Dyer, H. J. Quevedo, E. Gaul, A. C. Bernstein, M. Donovan, S. Kimura, M. Mazzocco, F. Consoli, R. DeAngelis, P. Andreoli, and T. Ditmire, Measurement of the Plasma Astrophysical S Factor for the ^{3}He$(d,p)^4$He Reaction in Exploding Molecular Clusters, Phys. Rev. Lett. **111**, 082502 (2013).

[22] W. Bang, M. Barbui, A. Bonasera, G. Dyer, H. J. Quevedo, K. Hagel, K. Schmidt, F. Consoli, R. DeAngelis, P. Andreoli, E. Gaul, A. C. Bernstein, M. Donovan, M. Barbarino, S. Kimura, M. Mazzocco, J. Sura, J. B. Natowitz, and T. Ditmire, Temperature Measurements of Fusion Plasmas Produced by Petawatt-Laser-Irradiated $D_2-{}^3$He or $CD_4-{}^3$He Clustering Gases, Phys. Rev. Lett. **111**, 055002 (2013).

[23] Y. Kim *et al.*, D-T gamma-to-neutron branching ratio determined from inertial confinement fusion plasmas, Phys. Plasmas **19**, 056313 (2012).

[24] C. Labaune *et al.*, Fusion reactions initiated by laser-accelerated particle beams in a laser-produced plasma, Nat. Commun. **4**, 2506 (2013).

[25] J. R. Zhao *et al.*, A novel laser-collider used to produce monoenergetic 13.3 MeV ^{7}Li(d, n) neutrons, Sci. Rep. **6**, 27363 (2016).

[26] C. Fu *et al.*, Laser-driven plasma collider for nuclear studies, Sci. Bull. **60**, 1211 (2015).

[27] J. R. Zhao *et al.*, Neutron yield enhancement in laser-induced deuterium-deuterium fusion using a novel shaped target, Rev. Sci. Instrum. **86**, 063505 (2015).

[28] R. Benattar, C. Popovics, and R. Sigel, Polarized light interferometer for laser fusion studies, Rev. Sci. Instrum. **50**, 1583 (1979).

[29] X. Liu *et al.*, Collisionless shockwaves formed by counter-streaming laser-produced plasmas, New J. Phys. **13**, 093001 (2011).

[30] S. Agostinelli *et al.*, GEANT4—a simulation toolkit, Nucl. Instrum. Methods Phys. Res. A **506**, 250 (2003).

[31] Z. S. Hartwig and P. Gumplinger, Simulating response functions and pulse shape discrimination for organic scintillation detectors with GEANT4, Nucl. Instrum. Methods Phys. Res. A **737**, 155 (2014).

[32] J. A. Frenje *et al.*, Absolute measurements of neutron yields from DD and DT implosions at the OMEGA laser facility using CR-39 track detectors, Rev. Sci. Instrum. **73**, 2597 (2002).

[33] J. D. Moody *et al.*, Multistep redirection by cross-beam power transfer of ultrahigh-power lasers in a plasma, Nat. Phys. **8**, 344 (2012).

[34] T. Morita *et al.*, Collisionless shock generation in high-speed counterstreaming plasma flows by a high-power laser, Phys. Plasmas **17**, 122702 (2010).

[35] Y. Yasutomo, K. Miyata, S.-I. Himeno, T. Enoto, and Y. Ozawa, A new numerical method for asymmetrical Abel inversion, IEEE Trans. Plasma Sci. **9**, 18 (1981).

[36] C. Chenais-Popovics *et al.*, Kinetic to thermal energy transfer and interpenetration in the collision of laser-produced plasmas, Phys. Plasmas **4**, 190 (1997).

[37] T. S. Ramazanov and S. K. Kodanova, Coulomb logarithm of a nonideal plasma, Phys. Plasmas **8**, 5049 (2001).

[38] R. Ramis, J. Meyer-ter-Vehn, and J. Ramírez, MULTI2D – a computer code for two-dimensional radiation hydrodynamics, Comput. Phys. Commun. **180**, 977 (2009).

[39] D. D. Ryutov, N. L. Kugland, M. C. Levy, C. Plechaty, J. S. Ross, and H. S. Park, Magnetic field advection in two interpenetrating plasma streams, Phys. Plasmas **20**, 032703 (2013).

[40] J. S. Pearlman, Faraday cups for laser plasmas, Rev. Sci. Instrum. **48**, 1064 (1977).

[41] G. M. Petrov and J. Davis, Energy and angular distribution of deuterons from high-intensity laser-target interactions, Plasma Phys. Controlled Fusion **50**, 015004 (2008).

[42] C. Bertulani, Nuclear astrophysics in storage rings, Nucl. Phys. A **626**, 187 (1997).